

Effect of flux creep on the temperature dependence of the current density in Y-Ba-Cu-O crystals

J. R. Thompson

*Solid State Division, Oak Ridge National Laboratory, Oak Ridge, Tennessee 37831-6061
and Department of Physics, University of Tennessee, Knoxville, Tennessee 37996-1200*

Yang Ren Sun

Department of Physics, University of Tennessee, Knoxville, Tennessee 37996-1200

L. Civale, A. P. Malozemoff,* M. W. McElfresh,† A. D. Marwick, and F. Holtzberg
IBM Thomas J. Watson Research Center, Yorktown Heights, New York 10598-0218

(Received 2 December 1991; revised manuscript received 8 April 1992)

Temperature-dependent critical current density and normalized flux-creep rate, together with the current dependence of the vortex pinning energy, were studied in as-grown and proton-irradiated Y-Ba-Cu-O crystals. A consistent interpretation is found within the collective-pinning or vortex-glass models.

I. INTRODUCTION

Ever since the recognition of the importance of giant flux creep¹ in high-temperature superconductors, efforts have been made to find a consistent picture of the temperature dependence of both the critical current density and the flux-creep rate. Remarkably, even after several years of intensive effort,²⁻⁷ reasonable results have only been attained in a narrow temperature range, for example, usually only below 20 or 30 K in YBa₂Cu₃O₇. Many experimental data consistently exhibit a quasiexponential temperature dependence for the critical current density J_c and a plateau in the normalized flux-creep rate S for temperatures above ~ 20 K. The anomalous plateau in the relaxation rate had been a puzzle, generating a variety of competing models involving distributions of pinning barrier heights⁸ or critical current densities⁹ or different current-density dependencies of the barrier height.^{4-7,10} Malozemoff and Fisher¹¹ pointed to a simple resolution of this problem in the context of vortex-glass^{12,13} or collective-pinning^{14,15} models. Nevertheless, the latter theories predict a temperature dependence for the critical current density J_c that does not have an explicitly exponential form, while our experiments and many earlier ones² consistently show a quasiexponential temperature dependence. It is thus important to clarify if this quasiexponential $J_c(T)$ is consistent with the above theories. Alternatively, an inability to explain this temperature dependence would raise serious questions about the applicability of these recent theoretical results.

As has already been pointed out,^{5,11} the key microscopic property that determines J_c and S is the current dependence of the vortex pinning potential $U(J)$. Recent theories and experiment have provided two specific expressions for $U(J)$, which will be tested in the following analysis. Complementing these developments and building on the formative work of Beasley, Labusch, and Webb,¹⁰ Maley *et al.*⁵ proposed an analysis of magnetic relaxation (flux-creep) studies that provides a direct

determination of $U(J)$, at least in the temperature regime $T \ll T_c$. In this paper we show that a consistent interpretation of both flux creep and current density *can* be found over a large temperature range up to about 60 K, if $U(J)$ follows the predictions of vortex-glass or collective-pinning theories. Moreover, we show that a direct determination of $U(J)$ provides further support for this interpretation. We also show that several competing theories fail. This work extends our earlier reports¹⁶⁻²⁰ on the magnetic properties of well-characterized YBa₂Cu₃O₇ crystals with controlled defect concentrations introduced by 3-MeV proton irradiation. The analysis applies successfully to both our as-grown and proton-irradiated Y-Ba-Cu-O crystals. The dependence of the fitting parameters on irradiation dose provides information about the irradiation-induced pinning sites.

II. EXPERIMENTAL ASPECTS

Several well-characterized, twinned single crystals of YBa₂Cu₃O₇, prepared using a flux-growth method described previously,²¹ were studied in these experiments. Sample masses were typically 100–400 μg , with thicknesses along the c -axis direction of 0.03 mm. As synthesized, the crystals had superconducting transition temperatures T_c near 93 K and transition widths ΔT_c of ~ 0.5 K, as measured by ac susceptibility. The crystals were irradiated at room temperature with 3-MeV protons at a flux of 3×10^{12} ions/(cm² sec), as described earlier.¹⁶ At the highest doses used in these experiments (10^{16} cm⁻²), T_c decreases about 1 K.

Measurements of the isothermal magnetization $M(H)$ were made for a set of temperatures T between 3 and 80 K, with fields $H \parallel c$ orientation, using a Quantum Design model MPMS superconducting quantum interference device (SQUID) based magnetometer. Applied magnetic fields up to 5.5 T were used. Samples were cooled to the desired temperature in zero applied field. Scan lengths of either 2 or 3 cm, providing a field uniformity of $\leq 0.05\%$

during measurement, were used, and temperature was stabilized to within ± 0.05 K of the target temperature before application of the magnetic field. An accuracy of better than $\pm 10^{-5}$ G cm³ was obtained. Due to a relaxation associated with the magnetometer itself (presumably with the SQUID measurement coils and shielding), magnetization measurements for the determination of J_c were made after a time delay adequately long to avoid this problem (typically 1 min after each field change). As we will see in detail below, the magnetization of the samples exhibited a significant time relaxation. Consequently, the combined effects of the waiting period and the finite time required for the application of magnetic field mean that we do not measure the idealized, creep-independent critical current density J_{c0} . Rather some smaller “apparent” critical current density $J_c(T)$, corresponding to a characteristic time of ~ 1 min, is obtained. This current actually is a long-lived persistent supercurrent, although convention labels it a “critical current.” The characteristic time of ~ 1 min is comparable to the initial time in the relaxation measurements.

The time relaxation of magnetization $M(t)$ for two crystals, both before and after proton irradiations with doses up to 10^{16} cm⁻², was studied using the SQUID magnetometer at $H=1$ T and various temperatures from 3 to 77 K. The sample was cooled to the desired temperature in zero field. Because of the large critical currents in the irradiated crystals, it was necessary first to cycle a crystal through a complete $M(H)$ cycle to -5 T before stopping at $+1$ T. This field cycling insured that the crystal was in the fully penetrated critical state and in the diamagnetic branch of the $M(H)$ loop. Thus, $M(t)$ was negative and decreased in absolute magnitude as a function of time t . For notational simplicity, all subsequent references to magnetization M denote its absolute value $|M|$. $M(t)$ was recorded over a time period ranging from 100 to 14 000 sec. For these relaxation studies, we define the origin of time $t=0$ as the effective time at which the system begins to relax from its idealized, creep-independent current density J_{c0} . Consequently the time of the first measurement of $M(t)$ is $t \approx 100$ sec. This time base absorbs into the quantity “ t ” both the settling time of the magnetometer and the effect of finite application rate of the magnetic field, which is equivalent to a (relatively short) shift of the time axis, as discussed in a later section.

III. EXPERIMENTAL AND MODEL RESULTS

Typical hysteresis loops have been shown earlier.^{16,19} Irradiation leads to a large increase in the width of the loop, that is, in the irreversible magnetization, which can be related to the current density J_c according to the Bean model.²² We use the formula²³ $J_c = 40M_{\text{irr}}/L$, where M_{irr} is one-half the width of the hysteresis loop at the given field; here $L = L_1[1 - (L_1/3L_2)]$ is a characteristic lateral dimension, where $L_1 \leq L_2$ are the sides of a rectangular crystal with the magnetic field applied perpendicular to that face. The units of J_c , M , and L are A/cm², G, and cm, respectively. We ignore any a - b anisotropy since the crystals were twinned.

Figure 1 shows on a semilogarithmic plot the temperature dependence of J_c for crystal no. 1 at $H=1$ T, both before and after irradiation to a dose of 10^{16} cm⁻². An approximately (“quasi-”) exponential decrease of J_c with T is observed in both cases for $T < 60$ K, followed by a more abrupt reduction at higher temperatures. This is consistent with many earlier reports.² A key observation about these data is that the relative enhancement of J_c with irradiation is temperature dependent, showing a 10-fold enhancement at 5 K and a 100-fold enhancement at 77 K. As we will show below, another crystal with different irradiation levels shows a similar progressive decrease of slope $d \ln(J)/dT$ with fluence of defect-creating ions.

A magnetic relaxation that was close to logarithmic as a function of time was observed at all of the temperatures measured, for both unirradiated and irradiated states, in the time range from 10^2 to 10^4 sec. At a longer time scale (up to 4×10^5 sec), deviations from logarithmic behavior become more evident, as have been reported elsewhere.²⁴ We have determined the normalized logarithmic decay rate $S = d \ln M(t)/d \ln(t)$, which in the time scale of the data is well approximated by $(1/M_i)dM/d \ln(t)$, where M_i is the (magnitude of) the initial irreversible magnetization measured at the beginning of the relaxation experiment. Since the current density and M decrease with time, S is inherently a negative quantity; in presenting and discussing experimental results, however, we shall always use the *magnitude* of S for convenience. Figure 2 shows the magnitude of S for crystal no. 1 as a function of T before and after irradiation.¹⁶ It is clear that irradiation changes S by less than 25% over the entire temperature range where measurements were reliable ($T=3$ –60 K), and that in both cases $S(T)$ exhibits a plateau in the range $20 \leq T \leq 60$ K.

Both the quasiexponential temperature dependence of J_c and the nonlinear temperature dependence of S are

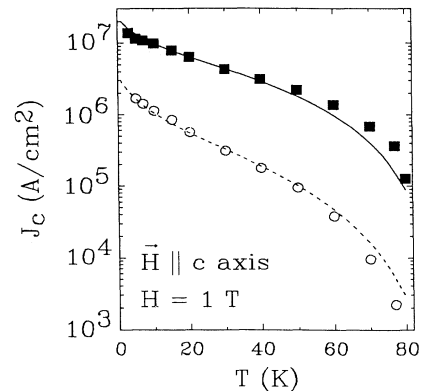


FIG. 1. Critical current density of YBa₂Cu₃O₇ crystal no. 1, as a function of temperature both before (○) and after (■) irradiation to a dose of 1×10^{16} H ions/cm². Lines show model results for $J_c(T)$ using Eq (10) from vortex-glass and collective-pinning theories. For this crystal, a current density of 10^6 A/cm² corresponds to a magnetization $M_{\text{irr}}=450$ G and magnetic moment $m_{\text{irr}}=6.9 \times 10^{-3}$ G cm³.

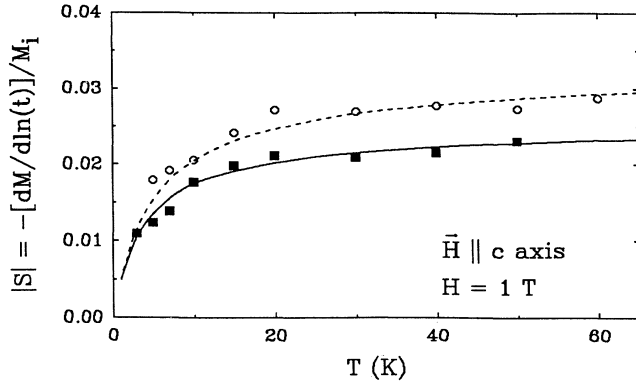


FIG. 2. Magnitude of the normalized magnetization decay rate S as a function of temperature, for crystal no. 1 before (○) and after (■) proton irradiation to a dose 1×10^{16} ions/cm². Lines are fits to Eq. (11) using parameters in Table I.

typical of all our samples. Next we trace the development of several models for this behavior.

The basic idea²⁵ is that the magnetic relaxation arises from thermal activation (flux creep) of flux lines or flux bundles over an average energy barrier U . This same effect leads to a reduction of the apparent critical current density. In high-temperature superconductors, the relaxation rate is so large¹ that the temperature dependence of J_c is dominated by flux-creep effects.

In the simplest model, first introduced by Anderson,²⁵ the net barrier is linearly reduced by the presence of a bulk current density, which, by Ampère's law, is necessarily related to the presence of a flux-line density gradient. Thus,

$$U(J) = U_0 [1 - (J/J_{c0})], \quad (1)$$

where U_0 and J_{c0} are, respectively, the temperature-dependent barrier height and critical current density in the absence of flux creep. Combining Eq. (1) with the Arrhenius relation (see the master rate equation, below) leads in the appropriate limit to the well-known flux-creep relation

$$J_c(T) = J_{c0} [1 - (T/U_0) \ln(t/t_{\text{eff}})], \quad (2)$$

where t_{eff} is an effective attempt time and energy U_0 is written in units of temperature. This equation displays the fact that the temperature and time dependence of J_c is a product of two factors: the factor J_{c0} that follows a BCS temperature dependence, and the quantity in brackets that gives the reduction due to flux creep. If U_0 is sufficiently small, this reduction can be very large. Equation (2) can be further differentiated to get the normalized relaxation rate⁸

$$S(T) = -T/[U_0 - T \ln(t/t_{\text{eff}})]. \quad (3)$$

Although Eqs. (2) and (3) are basic to the theory of flux creep, it is immediately apparent that they do not explain either the $J_c(T)$ or $S(T)$ data very well. While $J_c(T)$ decreases linearly at the lowest temperatures in agreement with Eq. (2), the equation obviously fails to reproduce the

quasiexponential behavior of the data. Even worse, Eq. (3) predicts an upward curvature of $S(T)$ which is entirely absent in the data.

One approach to overcome this discrepancy has been to invoke a distribution of either U_0 or J_{c0} . As was discussed in Ref. 11, the predicted $S(T)$ will depend on the details of the distribution and so it is difficult to reconcile these scenarios with the apparent universality of the data.

Another approach, which has been much discussed in the recent literature, is the possibility that a nonlinear dependence of U on J is responsible for these deviations. Beasley, Labusch, and Webb¹⁰ showed that in this case Eq. (2) generalizes to

$$J_c(T) = J_{c0} \{1 - [T/U^*(J_c)] \ln(t/t_{\text{eff}})\}, \quad (4)$$

where $U^*(J_c) = J_c |(\partial U/\partial J)_J| + U(J_c)$ is equivalent to U_0 in the Kim-Anderson picture, but is time dependent through $J_c(t)$. [This $U^*(J_c)$ is the same as the quantity U_0 in Fig. 1 of Beasley, Labusch, and Webb.¹⁰] These nonlinear models fall into two categories: those as in the Kim-Anderson treatment in which $U(J)$ approaches a finite limit when $J \rightarrow 0$, and those in which $U(J)$ diverges as $J \rightarrow 0$. Although the expression for S will depend on the particular $U(J)$, it is unlikely that nondiverging $U(J)$'s will produce a plateau in S . Indeed, we can write an approximate expression for S as

$$S = -T/[U^*(t^*) - T \ln(t/t_{\text{eff}})], \quad (5)$$

which will be valid within some restricted period of time around t^* . Since increases in T reduce J_c , then U^* can increase with temperature, provided $U(J)$ is concave upward. As seen from Eq. (5), a diverging $U(J)$ can lead to a $U^*(J_c)$ that overcomes the other T dependencies and reproduces the observed plateau.

A diverging $U(J)$ is hard to reconcile with the Anderson picture of a single particle in a well; however, it arises naturally as soon as long elastic vortices are considered.¹⁴ Based on transport data in Y-Ba-Cu-O thin films, Zeldov *et al.*²⁶ proposed a logarithmic dependence

$$U(J) = U_0 \ln(J_{c0}/J). \quad (6)$$

More recent evidence supporting this dependence comes from relaxation studies of Maley *et al.*^{5,7} Equation (6) leads to

$$J_c(T) = J_{c0} (t/t_{\text{eff}})^{-T/U_0} \quad (7)$$

and

$$S(T) = -T/U_0. \quad (8)$$

The prediction for $J_c(T)$ explains in a natural and elegant way the exponential dropoff with temperature, as has been pointed out recently by McHenry *et al.*,⁷ and it even accounts for the downward curvature on the $\ln J$ vs T plot in terms of the temperature dependence of U_0 . However, the logarithmic divergence is not strong enough to account for the decreasing slope of $S(T)$ and its plateau at intermediate temperatures.

While many other forms could be considered, we focus now on a form that has received increasing attention re-

cently, namely, an inverse power-law form that emerges from vortex-glass^{12,13} and collective-pinning–collective-flux-creep^{14,15} theories:

$$U(J) = (U_0/\mu)[(J_{c0}/J)^\mu - 1], \quad (9)$$

with characteristic exponent μ . Note that U depends implicitly on temperature through the quantities U_0 and J_{c0} . Originally, it was thought that vortex-glass and collective-pinning theories differed considerably, so the predictions of an identical power-law dependence for $U(J) \sim J^{-\mu}$ was remarkable. More recent thought suggests that the two formulations describe essentially the same physics,^{15(a)} although the relevant length scales are somewhat controversial. The similarity of underlying physics in the two theories applies particularly to the temperature-field regime well away from the “melting” line, which is the case that we study here. In adapting the results from vortex-glass theory, we have rescaled the energy prefactor (which is unspecified in the theory) by a factor of $1/\mu$. Consequently, the following equation (10) has, in the limit of small arguments, the same form as the Anderson-Kim expression and it is thus an “interpolation formula,” as described in Ref. 11. Before proceeding let us note the mathematical unity that Eq. (9) actually contains all of the $U(J)$ forms discussed. The KA case corresponds to $\mu = -1$, the Zeldov form to $\mu \rightarrow 0$, and the present cases to $\mu > 0$. Continuing with Eq. (9), one has

$$J_c(T) = J_{c0} / [1 + (\mu T / U_0) \ln(t/t_{\text{eff}})]^{1/\mu} \quad (10)$$

and

$$S(T) = -T / [U_0 + \mu T \ln(t/t_{\text{eff}})]. \quad (11)$$

As argued in Ref. 11, this last equation provides a natural explanation of the approximate universality in many studies of the value of the plateau in the temperature regime where $\mu T \ln(t/t_{\text{eff}})$ exceeds U_0 . However, the prediction for the temperature dependence of J_c in Eq. (10) has not yet been tested and does not appear to give an exponential temperature dependence.

To evaluate the temperature dependencies of J and S , we assume that J_{c0} and U_0 vary with temperature as

$$J_{c0}(T) = J_{c00} [1 - (T/T_c)^2]^n \quad (12)$$

and

$$U_0(T) = U_{00} [1 - (T/T_c)^2]^n. \quad (13)$$

These simple phenomenological forms approximate the temperature dependence expected of a BCS superconductor in the low-temperature limit because of the freezing out of quasiparticle excitations by the BCS energy gap. They exhibit a flat temperature dependence at low temperatures and fall off to zero approaching T_c . In our fits we have set exponent $n = \frac{3}{2}$, although other values do not give drastically different results. This choice, $n = \frac{3}{2}$, is appropriate for the current density, as seen by combining the relation from collective-pinning theory¹⁴ $J_{c0} \sim J_{\text{depairing}} \sim H_c / \lambda$ with standard approximations $\sim [1 - (T/T_c)^2]^{-1/2}$ for the temperature dependencies of

the coherence length ξ and penetration depth λ . To simplify and to avoid introducing additional variables, we use the same exponent $n = \frac{3}{2}$ to describe the T dependence of the energy U_0 . From collective-pinning theory, an alternate choice for the latter exponent would be $n = \frac{1}{2}$. For fitting Eq. (11) for $S(T)$ to the data, we adjust primarily the parameter $\mu \ln(t/t_{\text{eff}})$ that fixes the value of S at high temperature. To fit the temperature dependence of $J_c(T)$ with Eq. (11), we vary primarily the parameters J_{c00} , U_{00} , and μ . This process was iterated to obtain self-consistent parameters, since the same quantities appear in the expressions for $S(T)$ and $J_c(T)$. In this procedure, the objective is to model phenomenologically all the experimental results with a minimum set of physically reasonable parameter values. The lines in Figs. 1 and 2 are the results of fitting this model to the experimental data for crystal no. 1. The values of the fitting parameters are given in Table I. We have excluded explicit consideration of the data above 60 K, where both $J_c(T)$ and $S(T)$ appear to show new features, namely, a deviation from the quasiexponential behavior in $J_c(T)$ and a deviation from the plateau in $S(T)$, with S increasing¹⁶ with T .

At first sight, it is perhaps not surprising that we can get quite good fits to the data, given the number of parameters at our disposal. In fact, however, J_{c00} simply establishes the scale of J and the factor $\mu \ln(t/t_{\text{eff}})$ serves primarily to establish the plateau value of S . On the other hand, both the entire temperature dependence of J and the curvature of S at low temperatures depend strongly on U_0 . Combined, the four parameters describe concurrently the temperature dependence of both J_c and S . Before proceeding, we note that other reasonable values for the exponent “ n ” give similar results. For example, setting $n = \frac{1}{2}$ in Eq. (13) for $U_0(T)$ actually improves the fit for the irradiated case and leaves unchanged the values for μ , etc. In the corresponding unirradiated case, the modeling is slightly worse and yields values for μ and U_{00} that are $\sim 20\%$ smaller than those in Table I, with $J_{c00} \sim 35\%$ larger.

The quality of the previous fits gives strong evidence that the expression for $U(J)$ given by Eq. (9) is indeed a good approximation to the actual dependence. We now use the procedure proposed by Maley *et al.*⁵ to obtain directly $U(J)$. The analysis is based on the master rate equation¹⁰

$$dM/dt = (B\omega a / 2\pi r) \exp(-U/T),$$

TABLE I. Parameters used to model the temperature dependence of $J_c(T)$ and $S(T) = dM/M_i d \ln(t)$.

Crystal (no.)	Ion fluence 10^{16} H/cm ²	J_{c00} (MA/cm ²)	U_{00} (K)	μ	$\mu \ln(t/t_{\text{eff}})$
1	0	3.6	140	1.0	33
1	1	23	160	1.6	42
2	0	2.5	160	1.06	33
2	0.3	7.0	160	1.5	33
2	0.6	11	160	1.4	33

where B is the magnetic induction, ω is the attempt frequency for vortex hopping, a is the hopping distance, r is the sample radius, and energies are measured in K. Solving for the net pinning barrier U gives

$$U = -T[\ln(dM/dt) - C], \quad (14)$$

where $C = \ln(B\omega a/2\pi r)$. Since the Bean model gives $M \propto J_c$, Eq. (14) is an explicit expression for $U(J)$. If we were able to measure $M(t)$ in the whole range from $J_c \sim J_{c0}$ to $J_c \sim 0$, we could obtain the complete function $U(J)$. In reality, even the longest time relaxation data²⁴ allow us to probe only a tiny portion of $U(J)$. This limitation can be partially solved by using $M(t)$ data taken at various temperatures T_i . At each temperature, $M(t)$ will span a different portion of the $U(J)$ curve. Unfortunately, this analysis is complicated by the temperature dependencies of U_0 , J_{c0} , and perhaps the factor C . What we really obtain in this way is a collection of segments $U(J, T_i)$ that do not lie on a continuous curve. Nevertheless, this problem should not be very important for $T \ll T_c$. Figure 3 shows $U(J, T_i)$ as a function of J , as deduced from the $M(t)$ data using Eq. (14). Results are shown for both the unirradiated and irradiated cases for crystal no. 1. The various segments in each curve correspond to $M(t)$ values taken at different temperatures T_i . The factor C depends only logarithmically on the vortex hopping velocity and is assumed to be temperature independent over the range studied. Its value was chosen to make the segments at $T = 5, 7, 10$, and 15 K lie on a continuous curve, as expected for $T \ll T_c$. This criterion gave the values $C = 23$ and 16 for the unirradiated and irradiated cases, respectively. Note that the segments corresponding to higher values of T_i lie systematically and progressively below an extrapolation of the lower-temperature data. Recalling that the segments $U(J, T)$

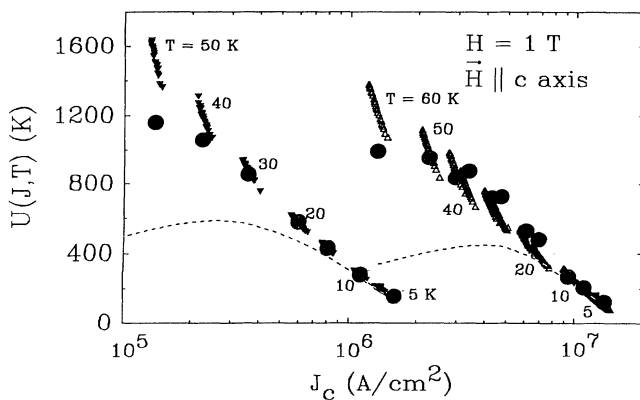


FIG. 3. The effective pinning energy $U(J, T_i)$ as a function of current density for crystal no. 1. Discrete line segments are derived from relaxation data at the temperatures shown, for the unirradiated crystal (semicontinuous curve at left) and irradiated with 10^{16} H ions/cm² (semicontinuous curve at right). The large circles are calculated from a power-law dependence on J [Eq. (9)], with temperature dependencies in Eqs. (12) and (13); see text. Dashed lines show the logarithmic form, Eq. (6), fitted to the respective low-temperature data.

depend on both J and T , one recognizes this progressive departure as a natural consequence of thermal weakening of the pinning potential.

We can now compare these data with the predictions for $U(J, T)$ given by the vortex-glass or collective-pinning model [Eq. (9)], using the parameters of Table I. The results are the large circles in Fig. 3. Let us emphasize the importance of Fig. 3 and the striking similarity of the two independent determinations. The segments are obtained directly from the experimental data using the master equation (14). No modeling is involved here and there are no assumptions regarding the magnitude of J_{c0} , U at $T = 0$, or any other quantities appearing in the modeling. In contrast, the circles are obtained from the $U(J)$ dependence of a specific model, with the parameters that fit the $J(T)$ and $S(T)$ predictions of that model. In calculating values for $U(J, T)$ from Eq. (9) (circles), we include exactly the same temperature dependencies for $J_{c0}(T)$ and $U_{00}(T)$ given in Eqs. (12) and (13). Thus, the primary influence of increasing temperature on $U(J, T)$ is included. Values of T for many segments appear in Fig. 3. Most notably, the agreement between the model and the “Maley” determinations of $U(J, T)$ is excellent at low temperatures, both for the unirradiated and irradiated cases. The slight deviations at high temperature can be a consequence of some residual temperature dependence from the factor C in Eq. (14). The overall agreement in Fig. 3 gives further evidence for the $U(J)$ form in Eq. (9) and for the self-consistency of the parameter values.

We can also compare the experimental $U(J, T_i)$ results with the logarithmic J dependence, Eq. (7). The results are shown in Fig. 3 as dashed lines for the unirradiated and irradiated cases. In constructing these curves, U_0 and J_{c0} were assumed to have the same BCS-like temperature dependencies given in Eqs. (12) and (13); however, the strengths U_{00} and J_{c00} were independently fitted to the data to best represent the low-temperature portion (5, 7, and 10 K) of the $U(J, T_i)$ curves. This procedure yielded the values $U_{00} = 400$ and 470 K, and $J_{c00} = 2.2$ and 17×10^6 A/cm², for the unirradiated and irradiated cases, respectively. Although the logarithmic model produces a good fit to the data at low temperatures, it begins to deviate significantly from the experimental results near 20 K, just where the plateau in $S(T)$ sets in.

Further evidence for the validity of the vortex-glass and collective-pinning pictures is provided by a similar analysis for a second crystal, which received intermediate proton fluences of 3 and 6×10^{15} ions/cm². Figure 4 presents the temperature dependence of $J_c(T)$ on a semi-log scale for crystal no. 2 at various irradiation levels, where the lines are model results. In Fig. 5 is shown the variation of S with T . To simplify the analysis and display additional generality, the same value for U_{00} , 160 K, has been used for all irradiation levels. The parameters used in fitting J_c and S in crystal no. 2 are given in Table I.

Overall, the model fits the experimental data in Figs. 1–5 quite well, even reproducing the slight upturn in J_c at low temperatures. For the data at high temperatures, $T > 60$ K, that were not explicitly included in the fit, the model reproduces qualitatively the increasingly rapid fall

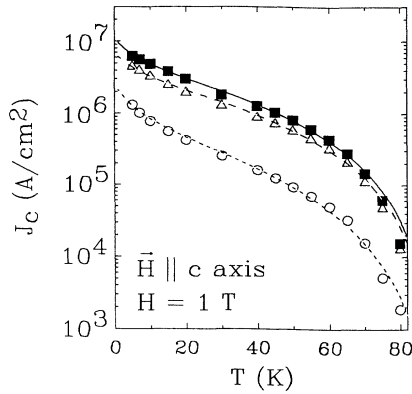


FIG. 4. Critical current density of crystal no. 2, as a function of temperature, prior to irradiation (\circ), irradiated with protons to a dose of 3×10^{15} ions/cm² (Δ), and irradiated with 6×10^{15} ions/cm² (\blacksquare). Lines are model results calculated with parameters in Table I. For this crystal, a current density of 10^6 A/cm² corresponds to an irreversible magnetization $M_{\text{irr}} = 1900$ G and magnetic moment $m_{\text{irr}} = 0.15$ G cm³.

of J_c with temperature.

Let us now consider the values for the individual parameters. For the exponent μ , the values used in this analysis are consistent with more precise determinations of μ obtained from detailed analyses of the time-dependent magnetization $M(t)$. The values $\mu \approx 1.0$ for the two unirradiated crystals are very similar to the result $\mu = 0.9$ observed in studies of c -axis aligned $\text{YBa}_2\text{Cu}_3\text{O}_{7-\delta}$ materials.²⁷ In the proton-irradiated crystals, the μ values used, (1.5 ± 0.1), lie well within the range of values observed^{18,24} in long-term flux-creep measurements on proton-irradiated Y-Ba-Cu-O crystal no. 1. It was shown there that the exponent μ is temperature dependent, following a trend that is consistent with the predictions¹⁴ of collective-pinning theory in the one-dimensional (1D) amorphous limit. In particular, the theory predicts μ values of $\frac{1}{7}$, $\frac{3}{2}$, and $\frac{7}{9}$ for progressively lower current densities where different vortex hopping

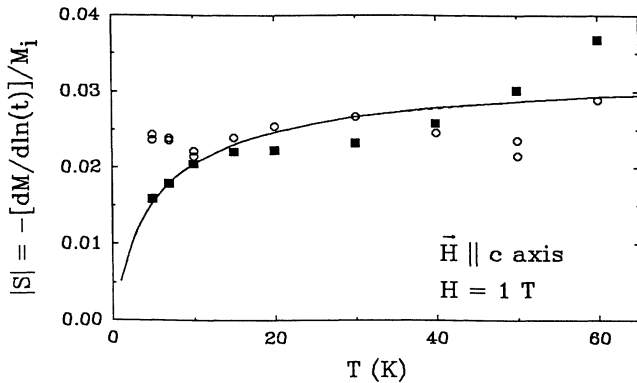


FIG. 5. Magnitude of normalized decay rate S vs temperature for sample no. 2, before (\circ) and after (\blacksquare) irradiation with 6×10^{15} H ions/cm².

processes prevail. For the irradiated crystals, the model values coincide remarkably well with the collective-pinning exponent for intermediate current densities, $\frac{3}{2}$. With the unirradiated crystals, the lower μ values are consistent with the trend in theoretical values. The predictions from vortex-glass theory are less specific, providing only that $\mu \leq 1$ in the region near the vortex-glass transition line, with no detailed predictions for the field-temperature region far below the melting line. The μ values in Table I should be taken as some average over the temperature range explored, although some details of the temperature variation remain an unresolved issue. These averages are defined to within approximately ± 0.1 .

Now consider the scale of pinning energy U_0 . For the present case, 1D pinning theory predicts that it should be the order of $(H_c^2/8\pi)(4\pi\xi_{ab}^2\xi_c/3)(\xi_{ab}/L_c)(a_0/L_c)^{1/5}$. (This is energy U_1 in the notation of Ref. 14.) Here L_c is the longitudinal correlation length, which can be estimated from the relation $(\xi_{ab}/L_c) \sim (J_{c0}/J_{\text{depairing}})^{1/2}$ and $a_0 \sim (\phi_0/B)^{1/2}$ is the spacing between vortices. For instance, this gives for irradiated crystal no. 1 at 5 K an energy $U_0 \sim 50$ K, in rough agreement with the experimental value in Table I. We emphasize that the theory¹⁴ gives only order-of-magnitude estimates for the pinning energy. We note also that the single-site energy $(H_c^2/8\pi)(4\pi\xi_{ab}^2\xi_c/3) \approx 130$ K is closer numerically to the values in Table I; however, such a picture of independent pinning sites is not consistent with the observed dependence of J_c on magnetic field, as the experimental J_c is independent of H at low temperatures.

Finally, note that the scale of current density J_{c0} is well behaved. The values are comparable for the two crystals before irradiation. They increase monotonically with ion fluence, as expected for a higher density of irradiation-induced defects. At an ion fluence $\sim 10^{16}$ protons/cm² giving an optimum current density, the value of $J_{c00} = 2.3 \times 10^7$ A/cm² is within a factor of ~ 15 of the depairing current density $J_{\text{depairing}} = 3.4 \times 10^8$ A/cm² $\propto H_c/\lambda_{ab}$. As discussed earlier, the experimental data and model values for J_c are depressed considerably below $J_{c0}(T)$, the critical current density in the absence of creep. Flux motion during two domains of time gives this depression: (1) during application of the magnetizing field at a finite sweep rate, the induced supercurrents are decaying,^{28,29} and (2) the currents decay further during the magnetometer settling time. Now, flux-creep annealing experiments³⁰ have shown that the time development of $M(t)$ and $J(t)$ is determined by the instantaneous current density J , but not by the route used to reach the given current density. Consequently, process (1) corresponds to a small shift in time, which in these studies can be absorbed into the time base. The net depression in supercurrent density is visualized in Fig. 6. This figure shows the temperature dependence of J_c for crystal no. 2 after irradiation with 6×10^{15} ions/cm², together with the calculated $J_{c0}(T)$ given by Eq. (12). For this case, flux creep depresses the measured current density by a factor of 2 at 5 K and a factor of 7 at 50 K.

It is noteworthy that the same theoretical treatment has given a good description of both unirradiated and ir-

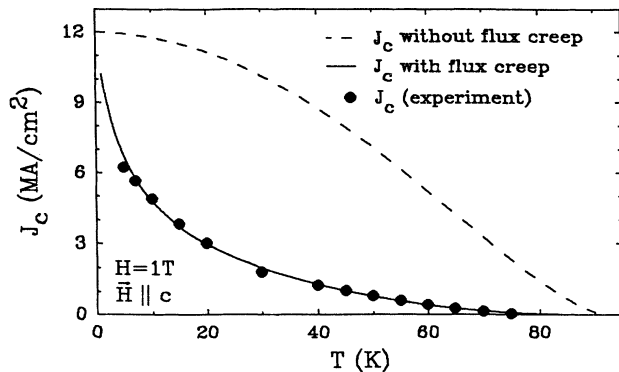


FIG. 6. Comparison of critical current densities vs temperature, showing experimental data (●) with the flux-creep model for $J_c(T)$ (solid line), calculated using $J_{c0}(T)$ (dashed line), the current density without flux creep. Data are for crystal No. 2; irradiated with 6×10^{15} ions/cm², with field of 1 T applied parallel to the c axis.

radiated crystals, with similar parameter values. The notable exception is the scale of current density J_{c00} . These features are consistent with the idea^{17,20} that the increased J_c in proton-irradiated Y-Ba-Cu-O crystals arises primarily from an increased density of pointlike defects. Indeed, we see that while the energy scale for an

individual pinning site is small (~ 100 K) corresponding to “weak pinning,” the *collective nature of many pins* can lead to quite high current densities ($\sim 10^7$ A/cm²) in case of an optimally dense array of pointlike sites.

Thus, we can conclude that among existing theories, the vortex-glass or collective-pinning formulas of Eqs. (9)–(11) provide the first successful phenomenological interpretation of the current dependence of pinning energy $U(J)$ and the temperature dependencies of critical current density $J_c(T)$ and normalized relaxation rate $S(T)$. Other competing theories seem inadequate. We regard the consistency of this analysis as a major new piece of evidence for these controversial theories.

ACKNOWLEDGMENTS

The authors wish to acknowledge many useful discussions with D. K. Christen and V. M. Vinokur. A portion of the work of J.R.T. and Y.R.S. was supported by the Science Alliance at The University of Tennessee, Knoxville and M.W.M. was supported in part by the Midwest Superconductivity Consortium through Department of Energy Grant No. DE-FG02-90ER45427. The research was sponsored by the Division of Materials Sciences, U.S. Department of Energy and technology development was funded by the U.S. Department of Energy Office of Advanced Utility Concept-Superconductor Technology Program, both under Contract No. DE-AC05-84OR21400 with Martin Marietta Energy Systems, Inc.

*Present address: American Superconductor Corporation, 149 Grove St., Watertown, MA 02172.

†Present address: Department of Physics, Purdue University, West Lafayette, IN 47907.

¹Y. Yeshurun and A. P. Malozemoff, Phys. Rev. Lett. **60**, 2202 (1988).

²A. P. Malozemoff, Mater. Res. Bull. **15**, 50 (1990); also in *Physical Properties of High Temperature Superconductors*, edited by D. Ginsberg (World Scientific, Singapore, 1989), p. 71.

³Y. Yeshurun, A. P. Malozemoff, and F. Holtzberg, J. Appl. Phys. **64**, 5797 (1988).

⁴Y. Xu, M. Suenaga, A. R. Moodenbaugh, and D. G. Welch, Phys. Rev. B **40**, 10882 (1989).

⁵M. P. Maley, J. O. Willis, H. Lessure, and M. E. McHenry, Phys. Rev. B **42**, 2639 (1990).

⁶B. M. Lairson, J. Z. Sun, J. C. Bravman, and T. H. Geballe, Phys. Rev. B **37**, 1008 (1990).

⁷M. McHenry, S. Simizu, H. Lessure, M. P. Maley, Y. C. Coulter, I. Tanaka, and H. Kojima, Phys. Rev. B **44**, 7614 (1991).

⁸C. W. Hagen and R. Griessen, Phys. Rev. Lett. **62**, 2856 (1989).

⁹J. Z. Sun, C. B. Eom, B. Lairson, J. C. Bravman, and T. H. Geballe, Phys. Rev. B **43**, 3002 (1991).

¹⁰M. R. Beasley, R. Labusch, and W. W. Webb, Phys. Rev. **181**, 682 (1969).

¹¹A. P. Malozemoff and M. P. A. Fisher, Phys. Rev. B **42**, 6784 (1990).

¹²M. P. A. Fisher, Phys. Rev. Lett. **62**, 1415 (1989).

¹³D. S. Fisher, M. P. A. Fisher, and D. A. Huse, Phys. Rev. B **43**, 130 (1991).

¹⁴M. V. Feigel'man, V. B. Geshkenbein, A. I. Larkin, and V. M.

Vinokur, Phys. Rev. Lett. **63**, 2303 (1989).

¹⁵M. V. Feigel'man and V. M. Vinokur, Phys. Rev. B **41**, 8986 (1990).

^{15a}V. M. Vinokur (private communication).

¹⁶L. Civale, A. D. Marwick, M. W. McElfresh, T. K. Worthington, A. P. Malozemoff, J. R. Thompson, and F. Holtzberg, Phys. Rev. Lett. **65**, 1164 (1990); L. Civale, A. D. Marwick, M. W. McElfresh, A. P. Malozemoff, and F. Holtzberg, in *High Temperature Superconductors: Fundamental Properties and Novel Materials Processing*, edited by D. K. Christen, J. Narayan, and L. F. Schneemeyer (Materials Research Society, Pittsburgh, 1990), p. 915.

¹⁷L. Civale, M. W. McElfresh, A. D. Marwick, T. K. Worthington, A. P. Malozemoff, F. Holtzberg, C. Feild, J. R. Thompson, D. K. Christen, and M. A. Kirk, in *Progress in High Temperature Superconductivity*, edited by J. L. Heiras, L. E. Sansores, and A. A. Valladares (World Scientific, Singapore, 1991), Vol. 31, p. 25.

¹⁸J. R. Thompson, Yang Ren Sun, D. K. Christen, H. R. Kerchner, A. P. Malozemoff, L. Civale, A. D. Marwick, L. Krusin-Elbaum, M. W. McElfresh, and F. Holtzberg, in *Physics and Materials Science of High Temperature Superconductors - II*, Vol. 209 of NATO Advanced Studies Institute Series E, edited by R. Kossowsky, B. Raveau, D. Wohlleben, and S. Patapis (Kluwer Academic, Dordrecht, 1992), p. 573.

¹⁹J. R. Thompson, Yang Ren Sun, A. P. Malozemoff, D. K. Christen, H. R. Kerchner, J. G. Ossandon, A. Marwick, and F. Holtzberg, Appl. Phys. Lett. **59**, 2612 (1991).

²⁰L. Civale, M. W. McElfresh, A. D. Marwick, F. H. Holtzberg, C. Feild, J. R. Thompson, and D. K. Christen, Phys. Rev. B

- 43, 13 732 (1991).
- ²¹D. L. Kaiser, F. Holtzberg, M. F. Chisholm, and T. K. Worthington, *J. Cryst. Growth* **85**, 593 (1987).
- ²²C. P. Bean, *Phys. Rev. Lett.* **8**, 250 (1962).
- ²³A. M. Campbell and J. E. Evetts, *Adv. Phys.* **21**, 199 (1972).
- ²⁴J. R. Thompson, Y. R. Sun, and F. Holtzberg, *Phys. Rev. B* **44**, 458 (1991).
- ²⁵P. W. Anderson and Y. B. Kim, *Rev. Mod. Phys.* **36**, 39 (1964).
- ²⁶E. Zeldov, N. M. Amer, G. Koren, A. Gupta, M. W. McElfresh, and R. J. Gambino, *Appl. Phys. Lett.* **56**, 680 (1990).
- ²⁷J. G. Ossandon, J. R. Thompson, D. K. Christen, B. C. Sales, Yang Ren Sun, and K. W. Lay, *Phys. Rev. B* **46**, 3050 (1992).
- ²⁸H. G. Schnack, R. Griessen, J. G. Lensick, C. J. van der Beek, and P. H. Kes, *Physica C* **197**, 337 (1992).
- ²⁹Yang Ren Sun, J. R. Thompson, D. K. Christen, J. G. Ossandon, Y. J. Chen, and A. Goyal, *Phys. Rev. B* **46**, 8480 (1992).
- ³⁰J. R. Thompson, Yang Ren Sun, A. P. Malozemoff, D. K. Christen, H. R. Kerchner, J. G. Ossandon, A. Marwick, and F. Holtzberg, *Appl. Phys. Lett.* **59**, 2612 (1991).